Amino Acids (2011) 40:895–911
DOI 10.1007/s00726-010-0728-7

ORIGINAL ARTICLE

Augmented O-GlcNAc signaling attenuates oxidative stress and calcium overload in cardiomyocytes

Gladys A. Ngoh · Lewis J. Watson · Heberty T. Facundo · Steven P. Jones

Received: 22 May 2010 / Accepted: 13 August 2010 / Published online: 27 August 2010

Abstract O-linked *β-N*-acetylglucosamine (O-GlcNAc) is an inducible, dynamically cycling and reversible post-translational modification of Ser/Thr residues of nucleo-cytoplasmic and mitochondrial proteins. We recently discovered that O-GlcNAcylation confers cytoprotection in the heart via attenuating the formation of mitochondrial permeability transition pore (mPTP) and the subsequent loss of mitochondrial membrane potential. Because Ca^{2+} overload and reactive oxygen species (ROS) generation are prominent features of post-ischemic injury and favor mPTP formation, we ascertained whether O-GlcNAcylation mitigates mPTP formation via its effects on Ca^{2+} overload and ROS generation. Subjecting neonatal rat cardiac myocytes (NRCMs, $n \geq 6$ per group) to hypoxia, or mice ($n \geq 4$ per group) to myocardial ischemia reduced O-GlcNAcylation, which later increased during reoxygenation/reperfusion. NRCMs ($n \geq 4$ per group) infected with an adenovirus carrying nothing (control), adenoviral O-GlcNAc transferase (adds O-GlcNAc to proteins, AdOGT), adenoviral O-GlcNAcase (removes O-GlcNAc to proteins, AdOGA), vehicle or PUGNAc (blocks OGA; increases O-GlcNAc levels) were subjected to hypoxia–reoxygenation or H_2O_2, and changes in Ca^{2+} levels (via Fluo-4AM and Rhod-2AM), ROS (via DCF) and mPTP formation (via calcein-MitoTracker Red colocalization) were assessed using time-lapse fluorescence microscopy. Both OGT and OGA overexpression did not significantly ($P > 0.05$) alter baseline Ca^{2+} or ROS levels. However, AdOGT significantly ($P < 0.05$) attenuated both hypoxia and oxidative stress-induced Ca^{2+} overload and ROS generation. Additionally, OGA inhibition mitigated both H_2O_2-induced Ca^{2+} overload and ROS generation. Although AdOGA exacerbated both hypoxia and H_2O_2-induced ROS generation, it had no effect on H_2O_2-induced Ca^{2+} overload. We conclude that inhibition of Ca^{2+} overload and ROS generation (inducers of mPTP) might be one mechanism through which O-GlcNAcylation reduces ischemia/hypoxia-mediated mPTP formation.

Keywords Mitochondria · Heart · Metabolism · Glucose

G. A. Ngoh · L. J. Watson · H. T. Facundo · S. P. Jones
Department of Physiology and Biophysics,
Diabetes and Obesity Center, Institute of Molecular Cardiology,
University of Louisville, Louisville, KY, USA

S. P. Jones (✉)
Department of Medicine, Institute of Molecular Cardiology,
University of Louisville, 580 South Preston St.,
Baxter II-321F, Louisville, KY 40202, USA
e-mail: Steven.P.Jones@Louisville.edu

Introduction

Ischemia–reperfusion injury is one of the major causes of morbidity and mortality in the western world. Calcium overload, oxidative stress and the more recently implicated involvement of endoplasmic reticulum (ER) stress characterize pathologic components of ischemia–reperfusion injury. Additionally, ischemia–reperfusion injury also causes a wide variety of functional and structural changes to the mitochondria (Halestrap 2004a; Crompton 1999; Crow et al. 2004; Di Lisa et al. 2001; Wang et al. 2005), including activation of the mitochondrial death pathway. The mitochondrial death pathway culminates with the formation of the mitochondrial permeability transition pore (mPTP), which represents a non-specific pore spanning both the outer and inner mitochondrial membranes that allow molecules <1.5 kDa to enter and exit the mitochondrial matrix. mPTP is activated by calcium overload

and reactive oxygen species (ROS), both of which are elevated in ischemia–reperfusion injury.

Manipulating the myocardium's response to ischemia–reperfusion is known to delay and/or reduce myocardial injury. Indeed, most cardioprotective interventions are known to mediate cytoprotection in part via attenuation of mPTP formation. Protein phosphorylation/dephosphorylation is one of the most studied biochemical aspects associated with these cardioprotective interventions. Interestingly, the novel post-translational sugar modification, O-linked *β-N*-acetylglucosamine (O-GlcNAc), has been shown in numerous studies and in different cell types to act as an inducible, cytoprotective stress response (Zachara et al. 2004; Ngoh et al. 2010). Our group (Ngoh et al. 2008, 2009a, b; Ngoh and Jones 2008; Jones et al. 2008) and others (Champattanachai et al. 2007, 2008; Yang et al. 2006; Zou et al. 2007, 2009) have shown that enhanced O-GlcNAcylation of proteins attenuates cardiomyocyte death and reduces infarct size in mice. Moreover, recent data from our laboratory reveal that O-GlcNAcylation is cardioprotective by attenuating mPTP formation (Ngoh et al. 2008, 2009a; Jones et al. 2008) and the activation of the maladaptive arm of the unfolded protein response (Ngoh et al. 2009b).

How O-GlcNAcylation mitigates mPTP formation is unknown. Therefore, we tested the hypothesis that O-GlcNAcylation reduces hypoxia-mediated mPTP formation via attenuating oxidative stress and Ca^{2+} overload in cardiomyocytes. We manipulated O-GlcNAc signaling and subjected myocytes to hypoxia–reoxygenation or oxidative stress to determine whether O-GlcNAcylation affected post-hypoxic or oxidative stress-induced ROS generation and Ca^{2+} overload. Our findings suggest that O-GlcNAcylation may attenuate mPTP formation by reducing Ca^{2+} overload and ROS generation.

Materials and methods

Murine in vivo ischemia–reperfusion

Three-month-old male C57BL6/J mice were subjected to in vivo coronary artery ischemia–reperfusion for assessment of O-GlcNAcylation levels according to a well-established protocol (Jones et al. 2008; Palazzo et al. 1998a, b, Jones et al. 1999a, b, 2000, 2001a, b, c, 2002, 2003a, b, 2004, 2005; Girod et al. 1999; Bueno et al. 2000; Hoffmeyer et al. 2000a, b; Condorelli et al. 2001; Scalia et al. 2001; Lefer et al. 2001; Sharp et al. 2002; Yang et al. 2003). Mice were anesthetized with intraperitoneal injections of ketamine hydrochloride (50 mg/kg) and sodium pentobarbital (50 mg/kg). The animals were then attached to a surgical board with their ventral side up. The mice were orally intubated with polyethylene (PE)-60 tubing connected to a mouse ventilator (Harvard Apparatus), and the tidal volume and breathing rate set by standard allometric equations. The mice were supplemented with 100% oxygen via the ventilator side port. Body temperature was maintained between 36.5 and 37.5°C using an electrically controlled rectal probe and a heat lamp. A left thoracotomy was performed using a thermal cautery, and the proximal left coronary artery was visualized with the aid of a dissecting microscope and completely occluded for 40 min with 7-0 silk suture mounted on a tapered needle (BV-1, Ethicon). After 40 min, the suture was removed and reperfusion was initiated and visually confirmed. The chest was closed in layers using 4-0 silk suture. The skin was closed using 4-0 nylon suture. Ketoprofen was given as analgesia prior to closing the chest. Upon recovery of spontaneous breathing, mice were removed from the ventilator, extubated and allowed to recover in a warm, clean cage supplemented with 100% oxygen.

Myocardial ischemic/non-ischemic zone determination

Following the 40-min period of ligation of the left coronary artery in mice as described above, reperfusion was initiated. After 0, 1, 4 and 24 h of reperfusion, mice were anesthetized with isoflurane. A tracheotomy was performed and mice were ventilated as described above. A catheter (PE-10 tubing) was placed in the common carotid artery to allow for Evans blue dye injection. A median sternotomy was performed, and the left coronary artery was re-ligated in the same location as before. Evans blue dye (1.2 ml of a 2% solution) was injected into the carotid artery catheter into the heart to delineate the ischemic zone from the non-ischemic zone. The heart was rapidly excised and serially sectioned along the long axis in 1-mm-thick sections. With the aid of a dissecting microscope, the non-ischemic and ischemic zones were separated and O-GlcNAcylation levels were assessed.

Neonatal rat cardiac myocyte isolation and culture

Neonatal rat cardiac myocytes (NRCMs) were isolated from 1 to 2-day-old Sprague-Dawley rats and cultured according to an established protocol (Ngoh et al. 2008, 2009a, b; Teshima et al. 2003a, b; Akao et al. 2001; Jones et al. 2003c). Cardiac myocytes in DMEM culture medium were plated on 35 mm glass bottom culture dishes at 75% density. During the first 4 days of culture, the medium contained the anti-mitotic BrdU (0.1 mmol/L) to inhibit any potential fibroblast growth in addition to 5% fetal bovine serum, penicillin/streptomycin and vitamin B_{12}. At 24 h prior to experimentation, the medium was changed to serum-free DMEM. All experiments were performed on at least four separate NRCM cultures.

Gene transfer

NRCMs were infected for 48 h with 100 MOI of replication-deficient adenoviruses carrying either the rat O-GlcNAc transferase gene (AdOGT), the rat O-GlcNAcase gene (AdOGA) or the green fluorescent protein (AdGFP; Vector Biolabs), as described previously (Ngoh et al. 2008; 2009a, b; Teshima et al. 2003b). The medium was changed to serum-free DMEM and myocytes were subjected to hypoxia–reoxygenation or challenged with H_2O_2. Sample size was equal to at least four per group per treatment.

Enzyme inhibition

NRCMs were treated overnight with *O*-(2-acetamido-2-deoxy-D-glucopyranosylidene) amino-*N*-phenylcarbamate (Ngoh et al. 2009a, b; Jones et al. 2008; Haltiwanger et al. 1998) (i.e., PUGNAc, 200 μmol/L), an inhibitor of OGA, or vehicle (0.1% ethanol), prior to the H_2O_2 challenge or hypoxia–reoxygenation. Sample size was equal to at least four per group per treatment.

In vitro hypoxia–reoxygenation injury in cardiac myocytes

Untreated cardiac myocytes were subjected to 6 h of hypoxia in Esumi lethal media in humidified hypoxic chambers (Billups-Rothenberg Inc.) as previously described (Ngoh et al. 2008, 2009b; Kelly et al. 2003). Following hypoxia, the media was changed to Esumi control media (Ngoh et al. 2008, 2009a) and culture dishes were reoxygenated for 0, 1 or 6 h in the modular incubator. Normoxic/aerobic controls were achieved by subjecting NRCMs to 6 h of normoxia and 6 h of reoxygenation in Esumi control media. Total cellular protein was isolated and immunoblotted for O-GlcNAc modification. Sample size was equal to six per group per treatment.

Induction of oxidative stress

Oxidative stress was induced in cultured NRCMs by adding 100 μmol/L H_2O_2, mixing and immediately imaging.

Protein expression

Total cellular proteins were isolated from NRCMs and heart sections, as previously described. As much as 50 μg of protein (according to Bradford assay) was applied to each lane of a 10% SDS-PAGE gel that was then electroblotted onto a PVDF membrane and probed for O-GlcNAc. A solution of 5% (v/v) reagent-grade non-fat milk in Tris-buffered saline was used for blocking, before incubating it in anti-O-GlcNAc antibody (1:1,000 CTD 110.6; Covance) overnight at 4°C. The blot was then incubated for 1 h with 0.05 μg/mL of goat anti-mouse IgM HRP-conjugated secondary antibody and detected with an enhanced chemiluminescent detection system (Pierce).

Enzymatic labeling of O-GlcNAc-modified proteins

O-GlcNAc-modified proteins were labeled using Invitrogen's Click-iT enzymatic labeling kit, as previously described (Ngoh et al. 2008). Briefly, detergents were precipitated out of 200 μg of whole cell lysate ($n = 6$ per group) using the chloroform/methanol precipitation method. The resulting pellets were then covered with lint-free paper and allowed to dry for 15 min in a fume hood. The dried pellets were resuspended in 40 μL of 1%, and allowed to cool on ice for 3 min. O-GlcNAc-modified proteins were then labeled with UDP-GalNAz (azide-modified UDP-*N*-acetylgalactosamine) using mutant β-1-4-galactosyltransferase at 4°C overnight. The next day, the GalNAz-labeled O-GlcNAc-modified protein mixture was precipitated using the chloroform/methanol precipitation method and resuspended in 50 μL of buffer containing 1% SDS and 50 mmol/L Tris–HCl (pH 8). The azide-labeled proteins were tagged with a fluorescent dye, TAMRA-alykne for 1 h at 4°C for the conversion of the azide group to a stable triazole conjugate. For 15 min, 25 mM DTT was added to stop the reaction and proteins were precipitated using the chloroform/methanol precipitation method. The dried, labeled protein sample was resuspended in SDS-PAGE buffer for electrophoresis. The gel was then imaged by excitation using a 532 nm laser on a TYPHOON 9400 imager.

Fluorescence microscopy

All fluorescent probes were purchased from Invitrogen. NRCMs were imaged in imaging/reoxygenation medium (DMEM with HEPES and minus phenol red and pyruvate). Images were captured using a Photometrics CoolSNAP ES camera attached to a Nikon-TE2000E2 fluorescence microscope with a T-PFS Perfect Focus Unit, all controlled with MetaMorph 6.3r2 software. The Perfect Focus System was used to prevent minute defocusing caused by changes over time during time-lapse imaging. Xcite 120 Fluor light source (level of 12%) was used and a Plan Apo 60xA/oil (NA = 1.4) objective was used for magnification. Neutral density filter setting was set at ND4 and binning of 2× for all image acquisition. Images were captured every 90 s for 60 min. Exposure duration, excitation filters and emission filters varied depending on the fluorescent dye, as mentioned below.

Assessment of reactive oxygen species production

ROS levels were assessed in NRCMs using time-lapse fluorescence microscopy by following the changes in

5-(and-6)-carboxy-2′,7′-dichlorodihydrofluorescein diacetate (DCF) fluorescence (Teshima et al. 2003b). NRCMs were loaded with 2 μmol/L DCF for 30 min at 37°C and the medium was changed to imaging/reoxygenation medium. For certain normoxic NRCM cultures, oxidative stress was induced and imaging was initiated immediately by excitation of DCF through 470/40 nm bandpass filter and emission through 522/40 nm bandpass filters. Exposure duration was set at 100 ms and all experimental groups were repeated in at least four separate isolations.

Assessment of calcium overload

Intracellular calcium overload was assessed in NRCMs using time-lapse fluorescence microscopy by following the changes in rhod-2 (Ngoh et al. 2009a; Teshima et al. 2003b, c) and fluo-4 fluorescence (Teshima et al. 2003c). For the hypoxia–reoxygenation study, NRCMs were loaded with 2 μmol/L rhod-2AM or 1 μmol/L fluo-4AM prior to hypoxia and imaging was initiated during reoxygenation. For oxidative stress studies, NRCMs were loaded with 1 μmol/L rhod-2AM (used to assess mitochondrial calcium) or 1 μmol/L fluo-4AM (used to assess cytosolic calcium) for 30 min at 37°C and the media was changed to imaging media. NRCMs were then treated with 100 μmol/L H_2O_2 and imaging was immediately initiated by sequentially exciting rhod-2 and fluo-4 through 560/28 and 470/40 nm bandpass filters, respectively. Emission was sequentially assessed through 646/38 nm (for rhod-2) and 522/40 nm (for fluo-4) bandpass filters. Exposure duration was set at 100 ms for both rhod-2 and fluo-4. All experimental groups were repeated in at least five separate NRCM cultures.

Assessment of mitochondrial permeability transition pore

Formation of mPTP was assessed in NRCMs using time-lapse fluorescence microscopy by following the changes in calcein fluorescence using a modified cold and warm loading protocol from Lemaster's group (Lemasters et al. 1998). NRCMs were loaded with 0.5 μmol/L calcein-AM for 180 min at 4°C. Next, NRCMs were loaded with 1 μmol/L MitoTracker Red FM at 37°C for 60 min. NRCMs were then washed and oxidative stress induced with 50 or 100 μmol/L H_2O_2. Imaging was initiated immediately afterward by excitation of calcein through 470/40 nm bandpass filter and emission through 522/40 nm bandpass filter. Excitation for MitoTracker Red was through a 560/28 nm bandpass filter, while emission was through 646/38 nm bandpass filter. Exposure duration was set at 50 ms for calcein and 100 ms for MitoTracker Red. Mitochondrial calcein fluorescence was determined using MetaMorph software in regions where both MitoTracker Red and calcein fluorescence colocalized. Mitochondrial calcein localization was assessed by measuring the standard deviation (SD) of the intensity of all green fluorescent pixels within the same region of interest using MetaMorph software. Each given region of interest had several mitochondria, each undergoing mPTP at different times. The SD reflected how the calcein fluorescence intensity of each mitochondrion varied from the average fluorescent intensity for that region of interest. A region of interest was defined by drawing a circle (43.61 μm^2) enclosing several mitochondria. SD is high when fluorescence is punctate and low when fluorescence is diffuse. All experimental groups were repeated in at least five separate isolations.

Statistical analyses

Data were analyzed using one-way ANOVA and/or Dunnett's t tests using GraphPad Prism 4 software. Data are reported as mean ± standard error of the mean with differences between treatment groups accepted as significant when $P < 0.05$.

Results

O-GlcNAc signaling changes during myocardial ischemia–reperfusion

We and others have shown that O-GlcNAcylation of proteins serves as an endogenously recruitable stress response (Ngoh et al. 2010). Moreover, studies from Chatham's group show that in isolated perfused rat hearts, simulated ischemia augments O-GlcNAcylation (Fulop et al. 2007; Liu et al. 2007a, b). Because nothing is known about in vivo changes in O-GlcNAcylation during myocardial ischemia–reperfusion injury, we directly addressed this question. We used the exogenous enzymatic labeling of O-GlcNAcylated proteins (click chemistry technique) to assess changes in O-GlcNAcylation levels in the ischemic (area at risk, $n = 4$ per group) and non-ischemic zones ($n \geq 4$ per group) of mice subjected to 40 min of myocardial ischemia (MI) via left coronary artery ligation or sham surgery and reperfused for 0 h (i.e., harvested after 40 min of ischemia without removing the ligature), 1, 4 or 24 h. Levels of O-GlcNAcylated proteins in the ischemic zone were reduced after 40 min of MI (group) compared to the sham group (Fig. 1b, $P < 0.05$, representative images shown in a). After 1 h of reperfusion, O-GlcNAcylation levels in the ischemic zone were ≈1.6-fold higher than sham and dropped to baseline levels after 4 or 24 h of reperfusion (Fig. 1b). Despite such changes in the ischemic zone of hearts from the MI group, there was no significant

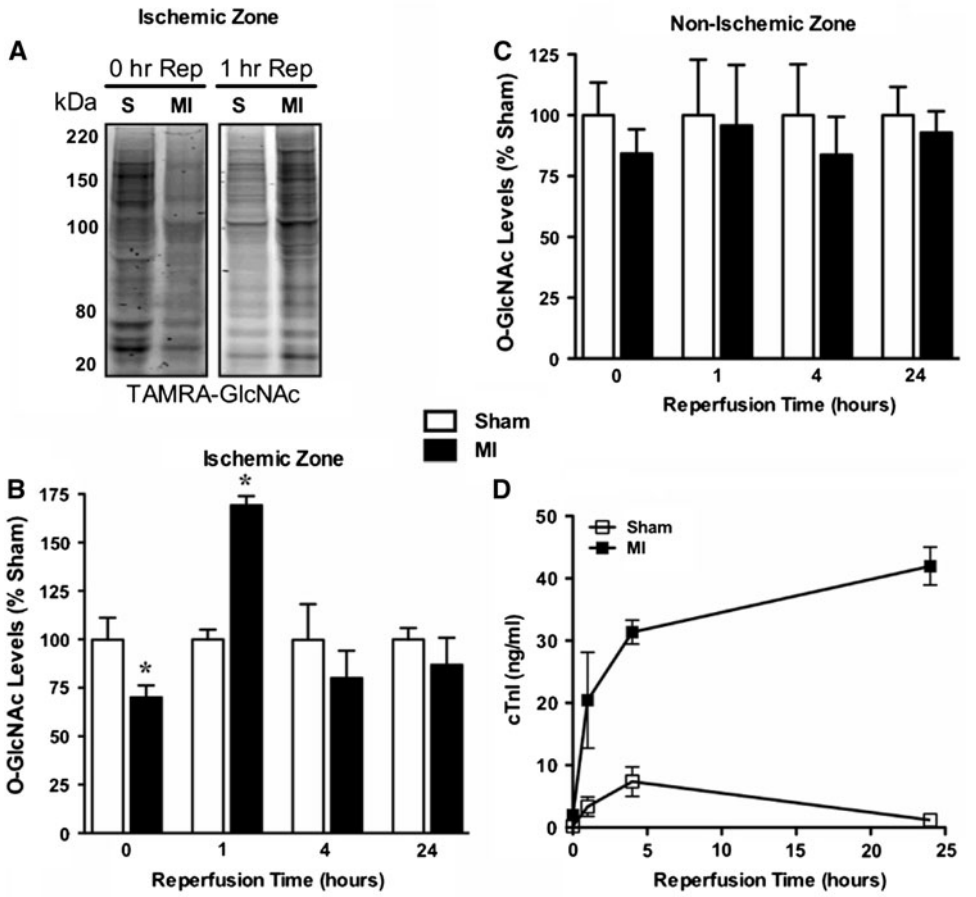

Fig. 1 Effects of ischemia–reperfusion injury on level of O-GlcNAcylation. Adult C57BL6 ($n = 4$–6 per group) mice were subjected to 40 min of ischemia and reperfused for the indicated time (in hours). **a** Representative TAMRA-GlcNAc gels for ischemic zone for time points with significant changes in O-GlcNAcylation. Ischemia induced significant decrement, while reperfusion for 1 h augmented O-GlcNAcylation. **b** Densitometric quantification of TAMRA-GlcNAc gels expressed as percent of sham for ischemic zones shows significant reduction in O-GlcNAcylation following 40 min of ischemia (0 h of reperfusion), augmented O-GlcNAcylation by 1 h of reperfusion and no change in O-GlcNAcylation by 4 and 24 h of reperfusion compared to sham. **c** There was no significant difference in O-GlcNAcylation in the non-ischemic zones of MI hearts compared with sham hearts at all reperfusion time points. **d** Ischemia induced troponin-I (cTnI) release. $^*P < 0.05$ versus sham

change in O-GlcNAcylated proteins in the non-ischemic (i.e., remote) zone from either MI or sham groups following ischemia or throughout reperfusion (Fig. 1c). To correlate the level of O-GlcNAcylated proteins to the amount of damage suffered by the myocardium, plasma was harvested prior to killing in all groups. Using an ELISA-based technique, plasma levels of cardiac troponin-I (cTnI, an intracellular protein released from cardiomyocytes following damage or death) were measured (Fig. 1d).

O-GlcNAcylation levels are altered following hypoxia–reoxygenation

To characterize the changes in O-GlcNAcylation during hypoxia and reoxygenation, we isolated NRCMs and subjected them to hypoxia and reoxygenation for 0, 1 or 6 h. Hypoxia significantly decreased O-GlcNAc levels compared to normoxia (Fig. 2a, $P < 0.05$, representative images shown in b). Upon reoxygenation, we observed a time-dependent increase in O-GlcNAc levels peaking after 6 h (Fig. 2a, representative image shown in b) and falling by 18 h of reoxygenation (data not shown).

Hypoxia damaged cardiac myocytes, as reflected by an increase in post-hypoxic LDH release compared to normoxia. Reoxygenation further exacerbated hypoxia-mediated myocyte injury, mirrored by the time-dependent increase in post-hypoxic LDH release for hypoxic myocytes compared to normoxia (Fig. 2c).

Manipulation of O-GlcNAc signaling alters oxidative stress

ROS are important contributors to ischemia–reperfusion injury and interventions that prevent a rise in ROS

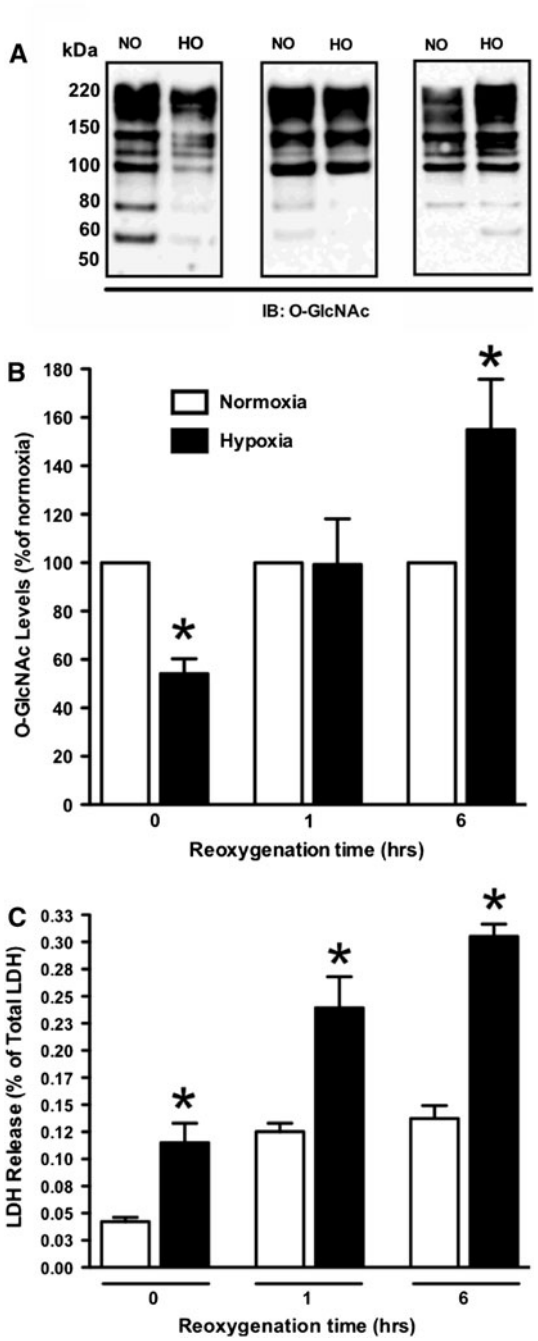

Fig. 2 Effects of hypoxia–reoxygenation on O-GlcNAc levels. Myocytes were subjected to hypoxia for 3 h and reoxygenated for 0, 1 or 6 h. O-GlcNAcylation levels were assessed on whole cell lysates or cell injury assessed by measuring post-hypoxic LDH release in the media. **a** Representative immunoblots of time course of O-GlcNAcylation levels in cardiac myocytes. **b** Densitometric quantification of O-GlcNAc immunoblots expressed as percent of normoxic control. **c** Hypoxia-induced cell injury according to post-hypoxic LDH release

generation reduce myocardial ischemia–reperfusion injury. Several studies have shown that the addition of antioxidants or ROS scavengers delay the onset or attenuate ischemia–reperfusion injury (Chi et al. 1989; Kilgore et al. 1994; Ambrosio et al. 1986). Therefore, we evaluated whether or not O-GlcNAc-mediated cardioprotection could be partially attributed to a reduction in oxidative stress-mediated ROS generation. NRCMs were treated with an adenovirus carrying the null, OGT or OGA genes, or treated with vehicle or PUGNAc. NRCMs were then subjected to 3 h of hypoxia or oxidative stress induced with 100 μmol/L hydrogen peroxide (H_2O_2). A change in DCF fluorescence during reoxygenation (or immediately following H_2O_2 treatment) indicates changes in ROS levels. Hypoxia induced a significant ($P < 0.05$) increase in ROS generation in NRCMs, reflected by increased DCF fluorescence (Fig. 3a). This effect was significantly ($P < 0.05$) attenuated by overexpression of OGT (Fig. 3a–c) or exacerbated by OGA overexpression. Additionally, inhibition of OGA with PUGNAc significantly reduced post-hypoxic ROS production (Fig. 3d–f).

Similarly, H_2O_2 treatment induced significant ROS generation, which was mitigated by OGT overexpression and worsened by OGA overexpression according to DCF fluorescence (Fig. 4a–c). The protective effects of augmented O-GlcNAc signaling on ROS levels were also observed when O-GlcNAc signaling was increased via pharmacologic OGA inhibition using PUGNAc (Fig. 4d–f). Despite the changes in ROS generation observed following hypoxia or peroxide treatment, there was no difference in ROS levels with either genetic (AdOGT or AdOGA) or pharmacologic (PUGNAc) manipulation of O-GlcNAc signaling during normoxia (data not shown).

Under normoxic conditions, basally generated ROS are efficiently detoxified by endogenous enzymatic antioxidants such as superoxide dismutase (SOD), glutathione peroxidase (GPX) and catalase (Cat) (McCord 2000; Lucchesi et al. 1989). However, during ischemia–reperfusion injury, there is excess ROS generation such that ROS generated exceeds the capacity of endogenous oxidant defense mechanisms to detoxify ROS and hence leading to deleterious ROS-mediated reactions. Accordingly, we ascertained whether altered O-GlcNAcylation affected baseline expression of the antioxidant enzymes SOD, GPX and Cat. qRT-PCR for Cat, GPX, SOD1 and SOD2 mRNA levels was performed on normoxic NRCMs treated with AdGFP, AdOGA, Vehicle or PUGNAc. OGT overexpression (AdOGT) did not significantly alter ($P > 0.05$) GPX, SOD1, SOD2, and Cat expression (Fig. 5a). Overexpression of OGA (AdOGA) did not significantly change GPX, SOD1 or SOD2 expression, though Cat was significantly reduced (Fig. 5a, $P < 0.05$). Likewise, inhibition of OGA with PUGNAc significantly increased Cat mRNA levels without changing SOD2 (Fig. 5b, $P < 0.05$).

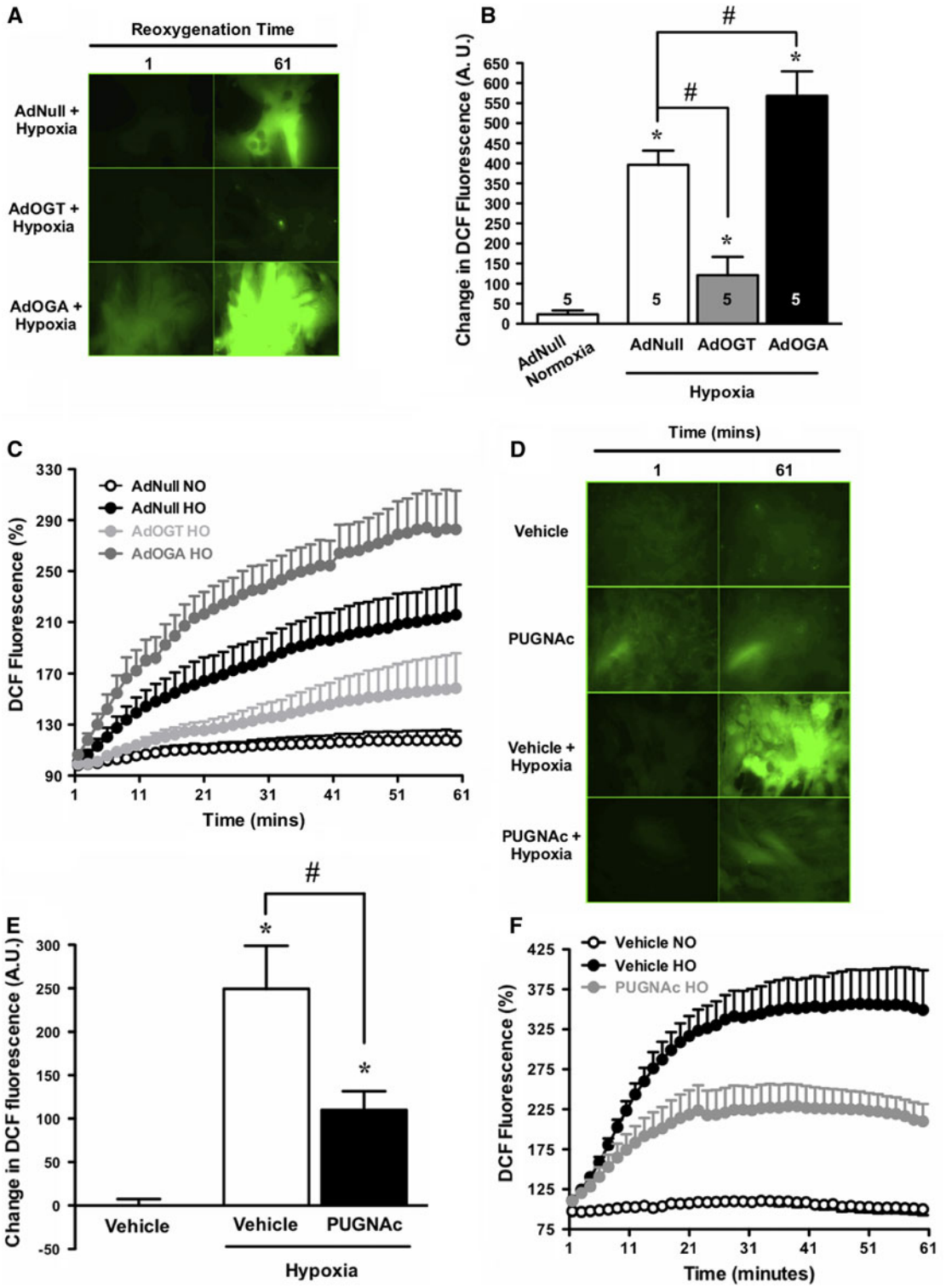

Fig. 3 Evaluation of ROS production in NRCMs treated with AdNull, AdOGT, AdOGA, vehicle or PUGNAc using DCF ($n = 6$ per group). Hypoxia-induced ROS production. AdOGT significantly attenuated, while AdOGA exacerbated, hypoxia-induced ROS production. OGA inhibition with PUGNAc also reduced post-hypoxic ROS generation. **a** Representative montage showing DCF fluorescence. **b** *Bar graph* showing the change in DCF fluorescent intensity between 1 and 61 min. **c** Quantitative changes in mean DCF fluorescence in NRCMs exposed to AdNull, AdOGT or AdOGA using time-lapse fluorescent microscopy. **d** Representative montage showing DCF fluorescence for vehicle versus PUGNAc. **e** *Bar graph* showing the change in DCF fluorescent intensity between 1 and 61 min for vehicle versus PUGNAc. **f** Quantitative changes in mean DCF fluorescence in NRCMs exposed to vehicle or PUGNAc using time-lapse fluorescent microscopy. $^{*}P < 0.05$ versus AdNull or vehicle, $^{\#}P < 0.05$ versus AdNull + hypoxia or vehicle + hypoxia

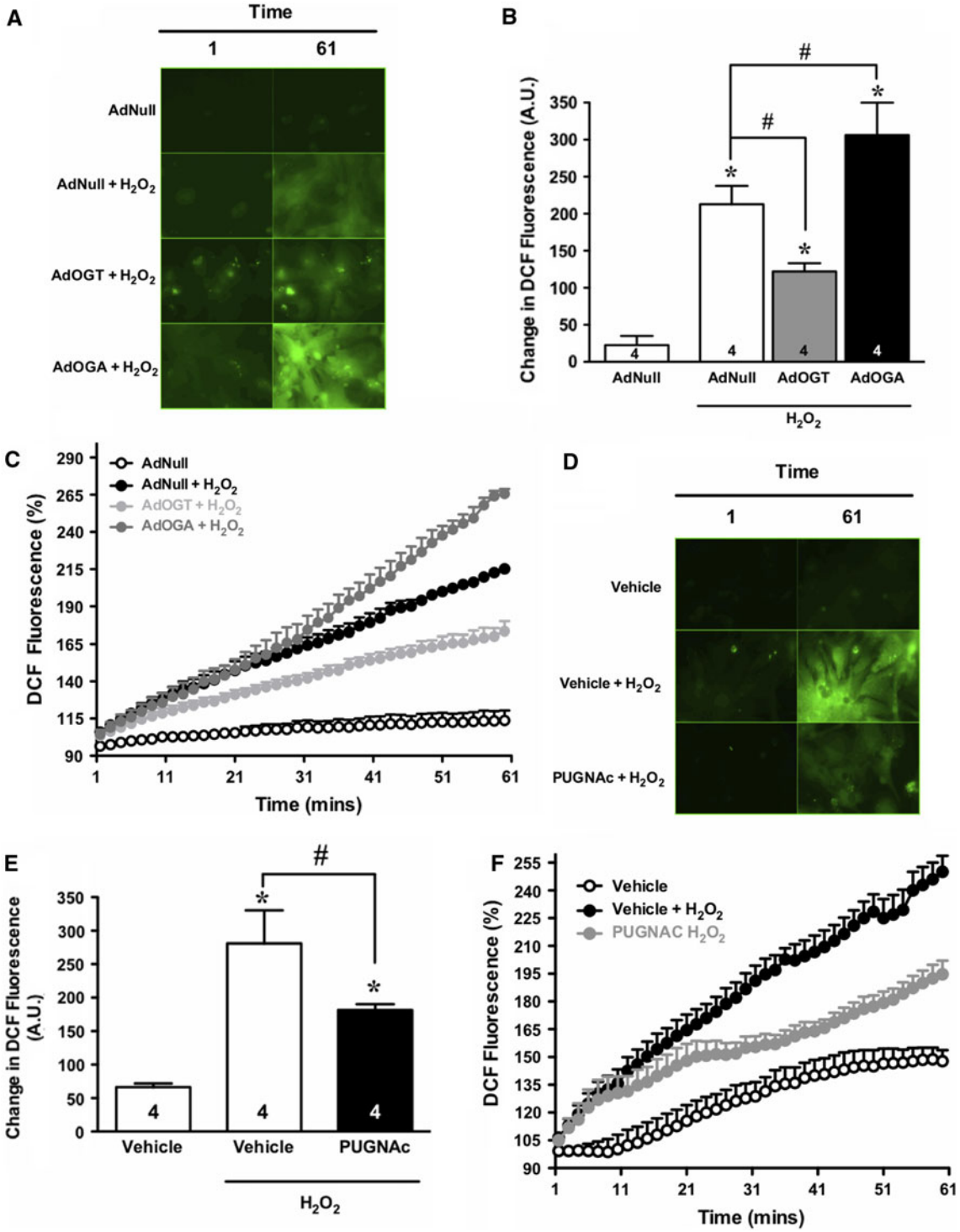

Fig. 4 Assessment of effects of manipulation of O-GlcNAc signaling on H_2O_2-induced ROS generation. NRCMs treated with AdNull, AdOGT, AdOGA, vehicle or PUGNAc were subjected to oxidative stress (with H_2O_2) and ROS levels measured using DCF ($n = 4$ per group). AdOGT significantly attenuated, while AdOGA exacerbated, H_2O_2-induced ROS production. OGA inhibition with PUGNAc also reduced H_2O_2-induced ROS production. **a** Representative montage showing DCF fluorescence for AdNull, AdOGT and AdOGA-treated NRCMs. **b** *Bar graph* showing the change in DCF fluorescent intensity between 1 and 61 min for AdNull, AdOGT and AdOGA-treated NRCMs. **c** Quantitative changes in mean DCF fluorescence in NRCMs exposed to AdNull, AdOGT or AdOGA using time-lapse fluorescent microscopy. **d** Representative montage showing DCF fluorescence for vehicle versus PUGNAc. **e** *Bar graph* showing the change in DCF fluorescent intensity between 1 and 61 min for vehicle versus PUGNAc. **f** Quantitative changes in mean DCF fluorescence in NRCMs exposed to vehicle or PUGNAc using time-lapse fluorescent microscopy. $^{*}P < 0.05$ versus AdNull or vehicle, $^{\#}P < 0.05$ versus AdNull + H_2O_2 or vehicle + H_2O_2

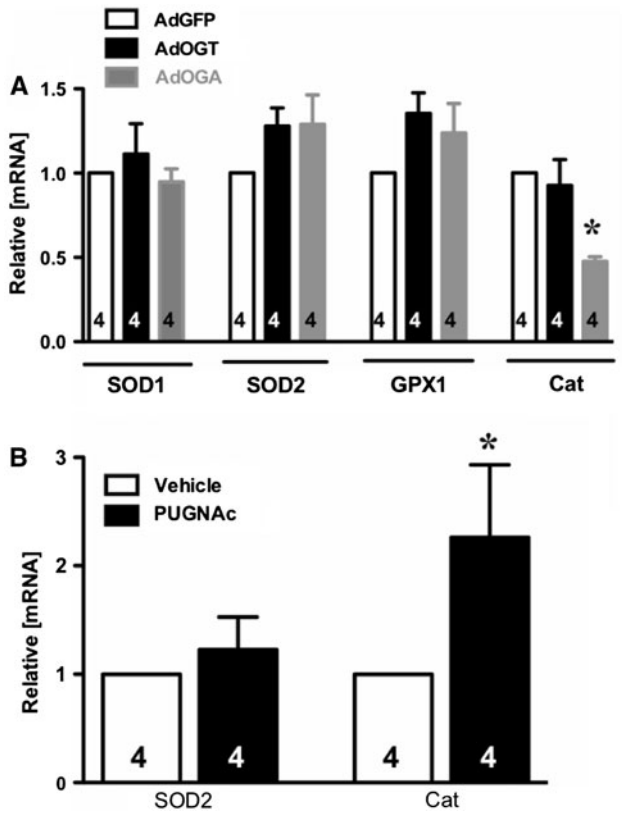

Fig. 5 Evaluation of anti-oxidant enzymes by qRT-PCR in NRCMs treated with AdGFP, AdOGT, AdOGA, vehicle or PUGNAc. **a** No change in mRNA levels of the anti-oxidant enzymes SOD1, SOD2, GPX or Cat occurred with either AdGFP or AdOGT. AdOGA did not affect SOD1, SOD2 or GPX, but significantly reduced Cat. **b** Inhibition of OGA with PUGNAc did not affect SOD2 levels, but increased Cat mRNA. $*P < 0.05$ versus AdGFP or vehicle

O-GlcNAc signaling attenuates hypoxic/oxidative stress-induced Ca^{2+} overload

Several studies have implicated Ca^{2+} overload as a key contributor to mitochondrial permeability transition leading to ischemia–reperfusion injury. Interventions that reduce or delay the rise in Ca^{2+} can block or delay myocardial death. In addition, inhibiting the rise in mitochondrial Ca^{2+} confers cardioprotection following acute ischemia (Murata et al. 2001; Girffiths and Halestrap 1995). Moreover, dysregulation of mitochondrial Ca^{2+} is known to induce mPTP formation (Hunter and Haworth 1979; Crompton et al. 1987). Accordingly, we assessed whether O-GlcNAcylation affects Ca^{2+} overload following hypoxia or oxidative stress in NRCMs ($n \geq 6$ per group). OGT overexpression did not alter baseline cytosolic or mitochondrial Ca^{2+} levels (data not shown), but significantly attenuated hypoxia-induced cytosolic (Fig. 6a–c) and mitochondrial (Fig. 6d–f) Ca^{2+} overload according to fluo-4 and rhod-2 fluorescence, respectively. The protective effect of augmented O-GlcNAcylation on both post-hypoxic cytosolic and mitochondrial Ca^{2+} overload was absent during the first 11 min of reoxygenation (Fig. 6c, f, respectively). Although fluo-4 and rhod-2 are generally accepted as cytosolic and mitochondrial calcium indicators (respectively), this is not a point of emphasis for the present study. Our point is to show two different indicators of *intracellular* calcium overload.

Augmented OGT expression significantly attenuated H_2O_2-induced cytosolic (Fig. 7a–c) and mitochondrial (Fig. 8a–c) Ca^{2+} overload. Although OGA overexpression did not affect H_2O_2 -induced cytosolic (Fig. 7a–c) or mitochondrial Ca^{2+} (Fig. 8a–c), OGA inhibition with PUGNAc significantly reduced H_2O_2-induced cytosolic (Fig. 7d–f) and mitochondrial (Fig. 8d–f) Ca^{2+} overload. To determine whether or not the lack of effect on H_2O_2-induced cytosolic and mitochondrial Ca^{2+} overload observed with OGA overexpression was because of maximally induced Ca^{2+} overload, a lower concentration (50 μmol/L) of H_2O_2 was used to induce oxidative stress. There was no difference in either cytosolic (Fig. 9a, c) or mitochondrial Ca^{2+} (Fig. 9b, c) overload induced by H_2O_2. Thus, the mechanism of exaggerated cell death in the context of elevated OGA activated may differ from loss of OGT activity (despite the fact that both treatments reduce O-GlcNAc levels).

O-GlcNAc signaling mitigates H_2O_2-induced mPTP formation

With mounting evidence suggesting that mPTP opening may be critical for the transition from reversible to irreversible myocardial ischemia–reperfusion injury (Crompton 1999), inhibition of mPTP formation likely represents an effective therapeutic approach in protecting the heart from reperfusion-induced damage. Indeed, direct and indirect inhibitors of mPTP opening have been shown to improve cardiac myocyte recovery after ischemia–reperfusion injury (Halestrap 2004b, 2006; Di Lisa 2001). Therefore, we investigated whether manipulation of O-GlcNAc signaling affected oxidative stress-induced mPTP opening using calcein in NRCMs. Fluorescent calcein is concentrated in the mitochondrial matrix and can be used to detect mPTP opening (Bernardi et al. 1999), as reflected by change from punctate to diffuse calcein fluorescence upon H_2O_2 exposure, despite there being no change in MitoTracker red fluorescence (Fig. 10a–c). H_2O_2 mediated mPTP opening was significantly delayed and attenuated by OGT overexpression (Fig. 10a), while OGA overexpression accelerated and worsened mPTP formation (Fig. 10a) compared to AdNull + H_2O_2, though not significantly. Additionally, OGA inhibition (PUGNAc) significantly mitigated mPTP formation (Fig. 10d–f) and CsA, a known mPTP blocker, significantly inhibited H_2O_2-mediated mPTP opening (data not shown).

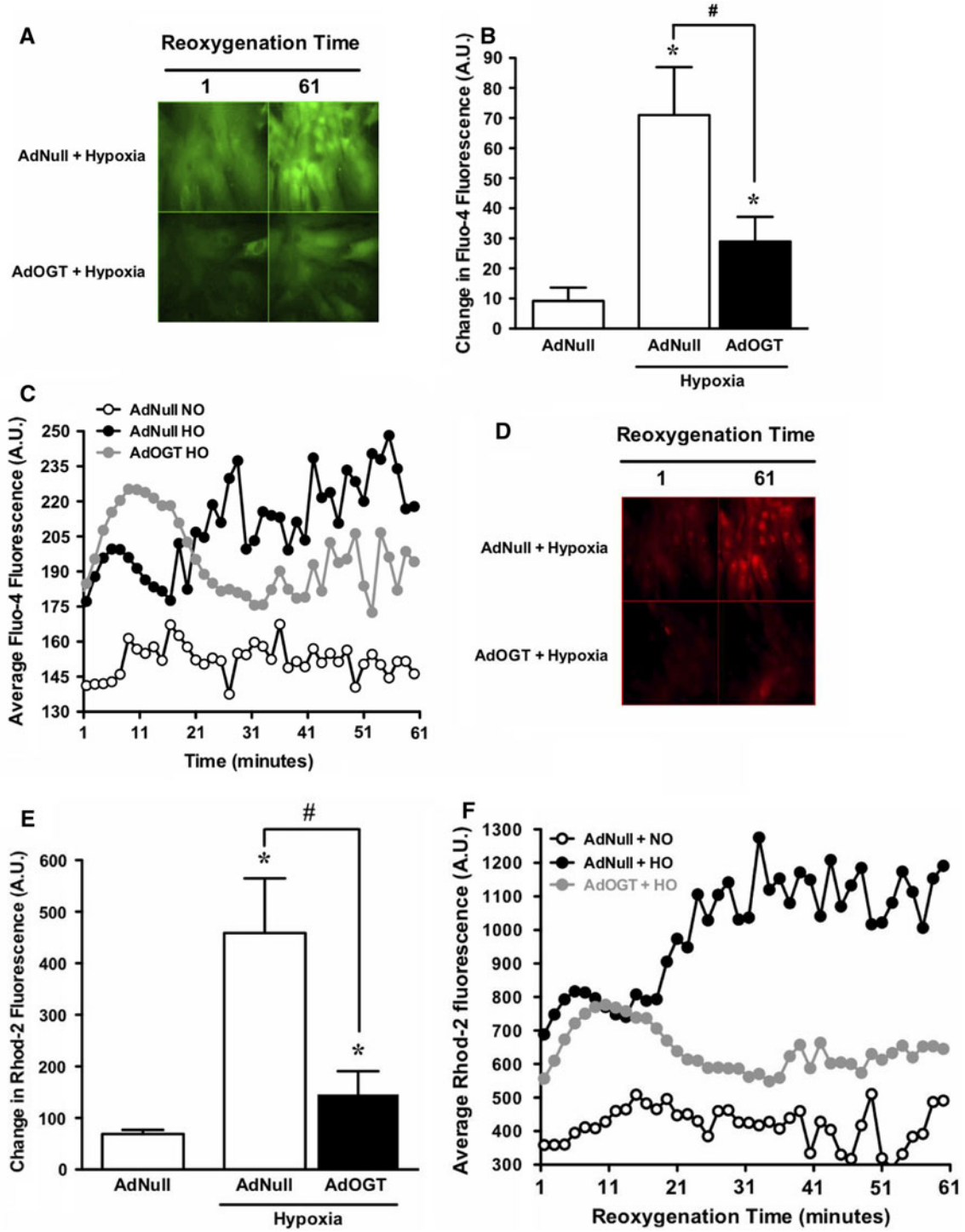

Fig. 6 Evaluation of calcium overload in NRCMs treated with AdNull or AdOGT and subjected to hypoxia/reoxygenation. AdOGT significantly attenuated cytosolic and mitochondrial Ca^{2+} overload. **a** Representative montage showing fluo-4 fluorescence for AdNull and AdOGT-treated NRCMs. **b** *Bar graph* showing the change in fluo-4 fluorescent intensity between 1 and 61 min for AdNull and AdOGT. **c** Time-lapse graph of mean fluo-4 fluorescence in NRCMs treated with AdNull or AdOGT and exposed to hypoxia/reoxygenation. **d** Representative montage showing rhod-2 fluorescence for AdNull or AdOGT-treated NRCMs. **e** *Bar graph* showing the change in rhod-2 fluorescent intensity between 1 and 61 min for AdNull or AdOGT-treated NRCMs. **f** Quantitative changes in mean DCF fluorescence in NRCMs exposed to AdNull or AdOGT using time-lapse fluorescent microscopy. $^{*}P < 0.05$ versus AdNull, $^{\#}P < 0.05$ versus AdNull + hypoxia/reoxygenation

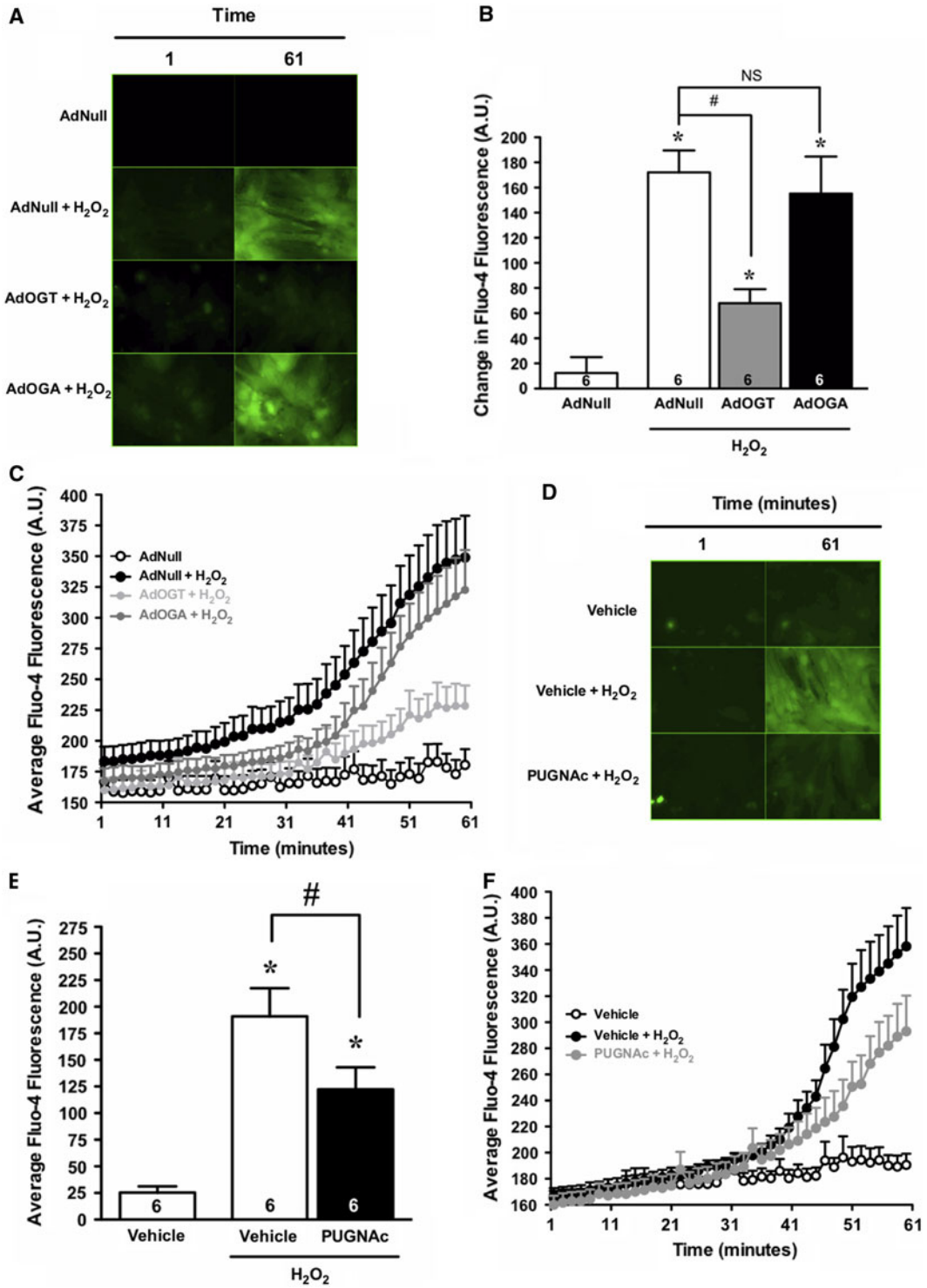

Fig. 7 Evaluation of calcium overload in NRCMs treated with AdNull, AdOGT, AdOGA, vehicle or PUGNAc and subjected to oxidative stress using fluo-4 ($n = 6$ per group). AdOGT significantly attenuated, while AdOGA did not affect H_2O_2-induced cytosolic Ca^{2+} overload. OGA inhibition with PUGNAc also reduced H_2O_2-induced cytosolic Ca^{2+} overload. **a** Representative montage showing fluo-4 fluorescence for AdNull, AdOGT and AdOGA-treated NRCMs. **b** *Bar graph* showing the change in fluo-4 fluorescent intensity between 1 and 61 min for AdNull, AdOGT and AdOGA-treated NRCMs. **c** Time-lapse graph of mean fluo-4 fluorescence in NRCMs treated with AdNull, AdOGT or AdOGA and exposed to H_2O_2. **d** Representative montage showing fluo-4 fluorescence for vehicle versus PUGNAc. **e** *Bar graph* showing the change in fluo-4 fluorescent intensity between 1 and 61 min for vehicle versus PUGNAc-treated NRCMs. **f** Quantitative changes in mean DCF fluorescence in NRCMs exposed to vehicle or PUGNAc using time-lapse fluorescent microscopy. $^{*}P < 0.05$ versus AdNull or vehicle, $^{\#}P < 0.05$ versus AdNull + H_2O_2 or vehicle + H_2O_2

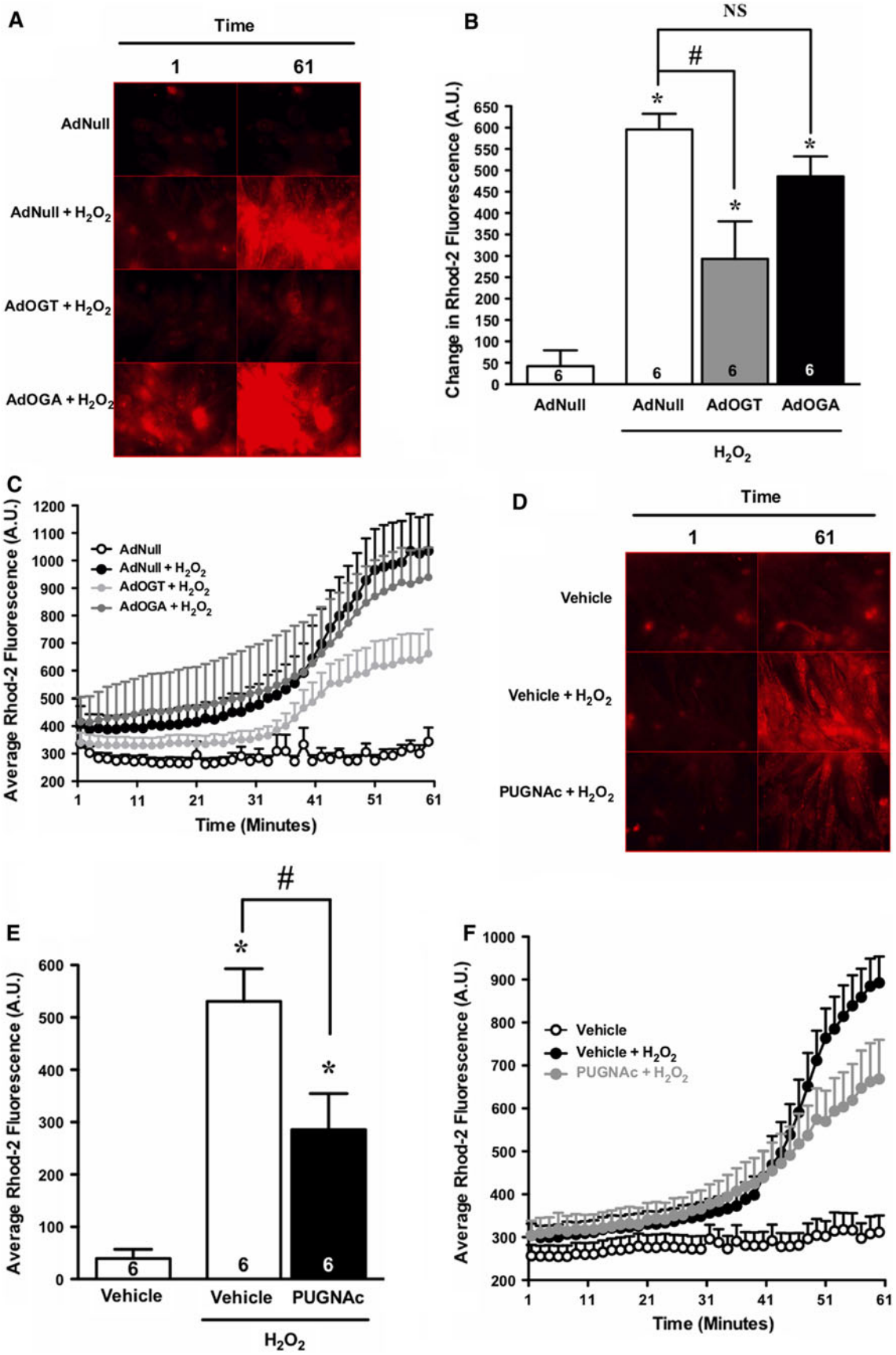
A
Time
1
61
AdNull
AdNull + H2O2
AdOGT + H2O2
AdOGA + H2O2
B
NS
#
*
Change in Rhod-2 Fluorescence (A.U.)
650
600
550
500
450
400
350
300
250
200
150
100
50
0
6
AdNull
AdNull
AdOGT
AdOGA
H2O2
C
Average Rhod-2 Fluorescence (A.U.)
1200
1100
1000
900
800
700
600
500
400
300
200
AdNull
AdNull + H2O2
AdOGT + H2O2
AdOGA + H2O2
1
11
21
31
41
51
61
Time (Minutes)
D
Time
1
61
Vehicle
Vehicle + H2O2
PUGNAc + H2O2
E
#
*
Average Rhod-2 Fluorescence (A.U.)
600
500
400
300
200
100
0
6
Vehicle
Vehicle
PUGNAc
H2O2
F
Average Rhod-2 Fluorescence (A.U.)
1000
900
800
700
600
500
400
300
200
Vehicle
Vehicle + H2O2
PUGNAc + H2O2
1
11
21
31
41
51
61
Time (Minutes)

◀ **Fig. 8** Evaluation of mitochondrial calcium overload in NRCMs treated with AdNull, AdOGT, AdOGA, vehicle or PUGNAc and subjected to oxidative stress using rhod-2 ($n = 6$ per group). AdOGT significantly attenuated, while AdOGA did not affect H_2O_2-induced mitochondrial Ca^{2+} overload. OGA inhibition with PUGNAc also reduced H_2O_2-induced mitochondrial Ca^{2+} overload. **a** Representative montage showing rhod-2 fluorescence for AdNull, AdOGT and AdOGA-treated NRCMs. **b** *Bar graph* showing the change in rhod-2 fluorescent intensity between 1 and 61 min for AdNull, AdOGT and AdOGA-treated NRCMs. **c** Time-lapse graph of mean rhod-2 fluorescence in NRCMs treated with AdNull, AdOGT or AdOGA and exposed to H_2O_2. **d** Representative montage showing rhod-2 fluorescence for vehicle versus PUGNAc. **e** *Bar graph* showing changes in rhod-2 fluorescent intensity between 1 and 61 min for vehicle versus PUGNAc-treated NRCMs. **f** Quantitative changes in mean DCF fluorescence in NRCMs exposed to vehicle or PUGNAc using time-lapse fluorescent microscopy. $^{*}P < 0.05$ versus AdNull or vehicle, $^{\#}P < 0.05$ versus AdNull + H_2O_2 or vehicle + H_2O_2

Discussion

The salient findings of the present study are as follows: (1) ischemia/hypoxia reduced, while reperfusion/reoxygenation augmented O-GlcNAcylated proteins, (2) OGT overexpression reduced hypoxia and oxidative stress-induced cytosolic and mitochondrial Ca^{2+} overload, (3) augmented O-GlcNAcylation (AdOGT and PUGNAc) attenuated hypoxia and oxidative stress-induced ROS production, while diminished O-GlcNAcylation (AdOGA) exacerbated it, (4) enhanced O-GlcNAcylation suppressed mPTP opening in cardiac myocytes following oxidative stress, while reduced O-GlcNAcylation sensitized to it. These results demonstrate that a potential mechanism through which O-GlcNAcylation mitigates mPTP is by blocking Ca^{2+} overload and ROS generation.

In addition to its roles in signal transduction and in regulation of redox cell signaling, ROS generation contributes to myocardial ischemia–reperfusion injury (Lefer and Granger 2000). Enhanced O-GlcNAcylation of proteins (AdOGT and PUGNAc) mitigated both hypoxia- and oxidative stress-mediated ROS generation, while AdOGA exacerbated hypoxia-induced ROS generation. One might conjecture that O-GlcNAcylation attenuates ROS generation by upregulating the expression and/or activity of the antioxidant enzymes Cat, GPX and SOD. Moreover, forkhead box O1 (FoxO1), a regulator of the transcription of the oxidative stress responsive enzymes Cat and MnSOD (SOD2), was shown recently to be O-GlcNAc modified (Housley et al. 2009). O-GlcNAcylation of FoxO1 activates FoxO1 and can in turn lead to activation of transcription of oxidative stress response enzymes, Cat and MnSOD. Here, we show that neither augmented (AdOGT and PUGNAc) nor diminished (AdOGA) O-GlcNAcylation significantly altered baseline mRNA levels of SOD or GPX. However, inhibition of OGA (PUGNAc) augmented, while overexpression of OGA reduced, baseline Cat mRNA. The alteration in Cat expression with OGA manipulation partially explains the exacerbated post-hypoxic ROS generation seen with OGA

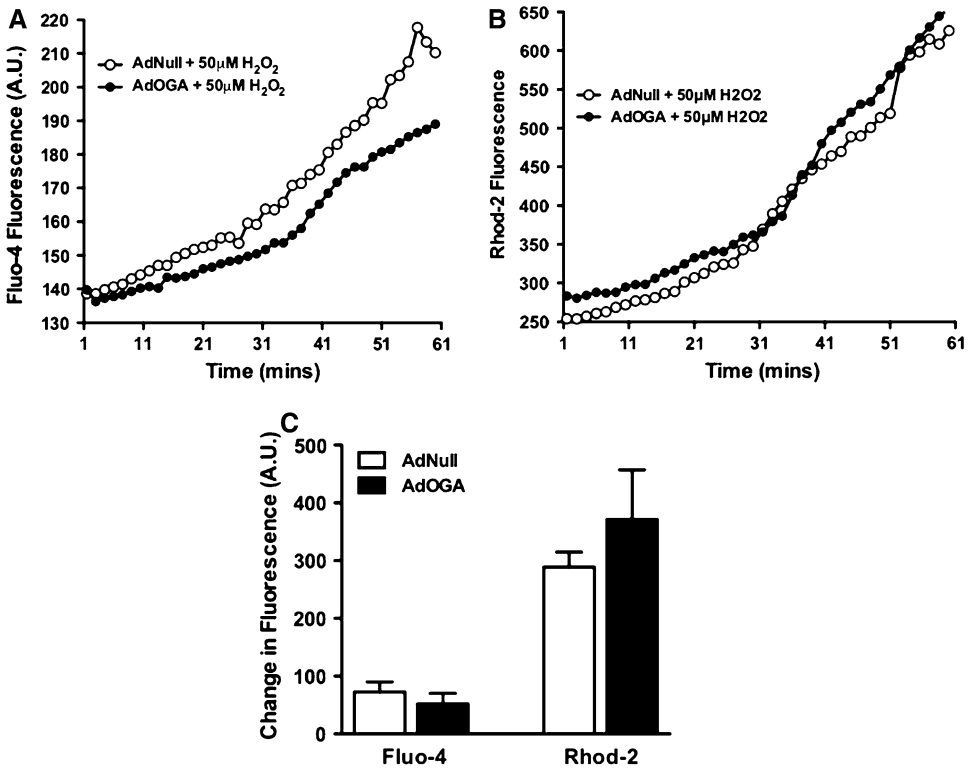

Fig. 9 Assessment of peroxide-induced calcium overload in NRCMs exposed to a low (50 μmol/L) concentration of H_2O_2. **a** Cytosolic calcium levels as shown by fluo-4 fluorescence. **b** Mitochondrial calcium levels as shown by rhod-2 fluorescence. **c** Change in fluorescence in both fluo-4 and rhod-2

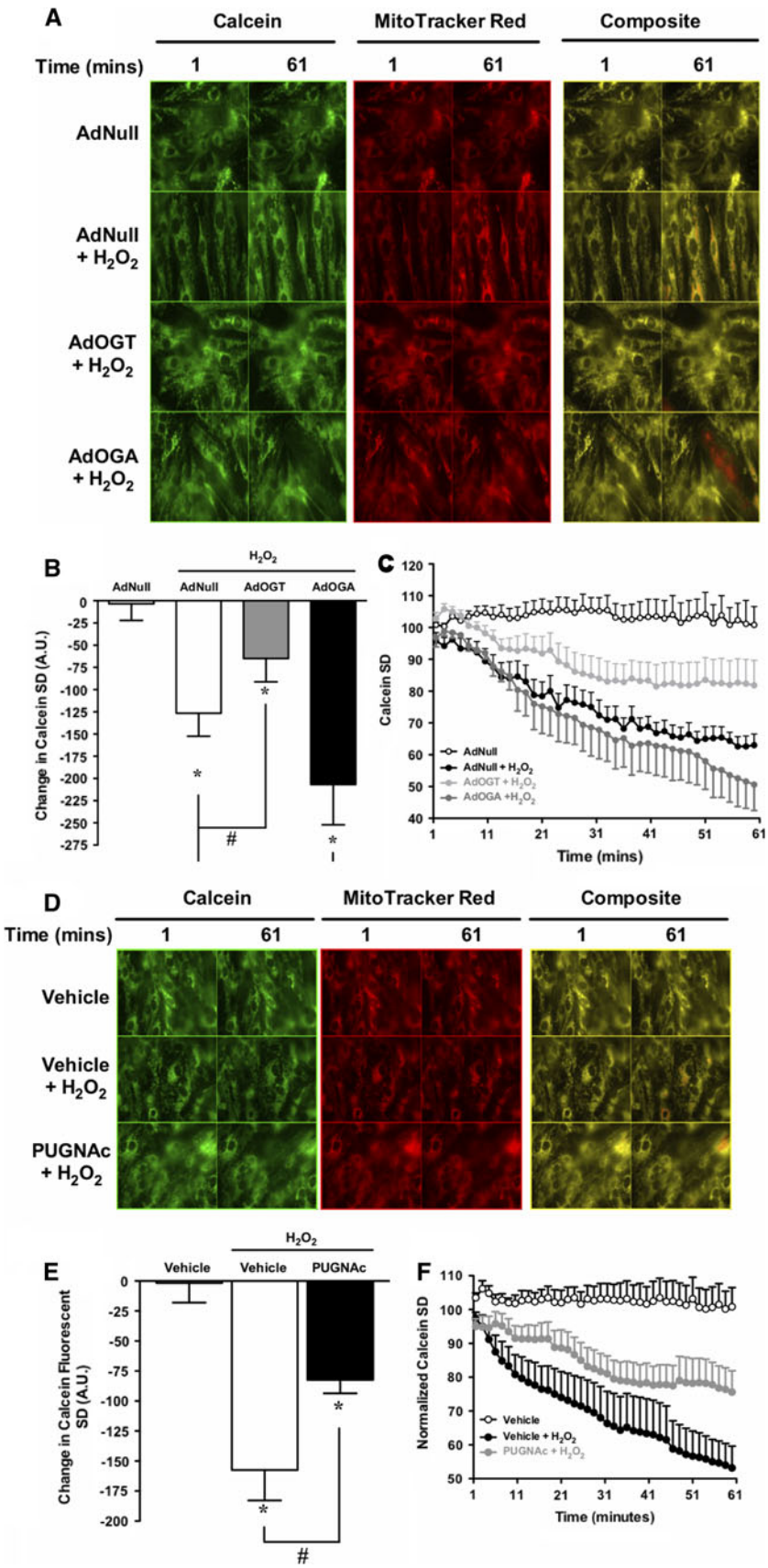

Fig. 10 Assessment of sensitivity to formation of mitochondrial permeability transition pore (mPTP) in NRCMs treated with AdNull, AdOGT, AdOGA, vehicle or PUGNAc prior to H_2O_2 treatment using calcein and MitoTracker Red. Loss of calcein fluorescence was used to indicate mPTP ($n \geq 6$ per group). H_2O_2 treatment induced mPTP opening, which was attenuated by OGT overexpression or exacerbated by OGA overexpression according to: **a** representative montages, **b** quantitative *bar graph* showing the change in calcein fluorescent intensity SD between 1 and 61 min, and **c** graph showing time-dependent changes in mean calcein fluorescence intensity standard deviation in NRCMs treated with AdNull, AdNull + H_2O_2, AdOGT + H_2O_2 and AdOGA + H_2O_2. OGA inhibition with PUGNAc also mitigated mPTP formation according to: **d** representative montages of calcein fluorescence, **e** quantitative *bar graph* showing the change in calcein fluorescent intensity SD between 1 and 61 min, and **f** *graph* showing time-dependent changes in mean calcein fluorescence intensity standard deviation in NRCMs treated with vehicle, vehicle + H_2O_2, and PUGNAc + H_2O_2. $^{*}P < 0.05$ versus AdNull or vehicle, or $^{\#}P < 0.05$ versus AdNull + H_2O_2 or vehicle + H_2O_2

overexpression and reduced ROS generation with OGA inhibition. Likewise, OGA inhibition reduced oxidant stress-induced ROS production but OGA overexpression surprisingly did not seem to have a negative effect in the same system.

Another important finding in the present study is that enhanced O-GlcNAcylation attenuates post-hypoxic and oxidative stress-mediated Ca^{2+} overload. These data support previous findings by our group showing that augmented O-GlcNAcylation, via inhibition of OGA (PUGNAc), mitigated hypoxia-induced calcium overload, while reduction of O-GlcNAcylation, via OGA overexpression, worsened hypoxia-induced Ca^{2+} overload. Additionally, Nagy et al. (2006) previously showed that enhanced O-GlcNAcylation with glucosamine treatment blocked angiotensin II-induced cytosolic Ca^{2+} overload in neonatal cardiomyocytes and that such beneficial effects were dependent on OGT.

How O-GlcNAcylation attenuates Ca^{2+} overload in acute stress is unknown. Because a primary source for the rise in intracellular Ca^{2+} during/following ischemia or hypoxia might be via reverse functioning NCX, it is possible that enhanced O-GlcNAcylation levels mitigate cytosolic Ca^{2+} overload via indirect effects on an upstream activator of NCX or direct effect on NCX. Other possible mechanisms may be enhanced SERCA2a activity and/or decreased phospholamban binding to SERCA2a. Such hypotheses remain to be tested but are certainly worthy of investigation.

Enhanced O-GlcNAcylation also attenuates mitochondrial Ca^{2+} overload. Ca^{2+} likely enters the mitochondria via the mitochondrial uniporter. Because there may exist a mitochondrial OGT isoform (mOGT), which is thought to be membrane bound, it is possible that mOGT interacts with the mitochondrial Ca^{2+} uniporter preventing Ca^{2+} uptake into the mitochondria. Therefore, understanding how O-GlcNAcylation affects Ca^{2+} handling in the heart is critical to the determination of how O-GlcNAcylation modulates mPTP.

mPTP appears to be critical for the transition from reversible to irreversible myocardial ischemia–reperfusion injury (Crompton 1999). ROS and Ca^{2+} activate mPTP and both of these are elevated during MI and reperfusion. Numerous cardioprotective pathways work primarily by inhibition of mPTP formation directly or indirectly by preventing the conditions that promote mPTP formation. The present study demonstrates that augmented O-GlcNAcylation (AdOGT or PUGNAc) attenuates mPTP formation in NRCMs, while diminished O-GlcNAcylation sensitizes NRCMs to mPTP formation. These data support previous findings by our group showing that enhanced O-GlcNAcylation reduces cardiac mitochondria to mPTP formation, while diminished O-GlcNAcylation sensitizes them to mPTP formation. Based on the present data, it is possible that one way through which O-GlcNAcylation mitigates mPTP formation might be through indirect means by attenuation of Ca^{2+} overload and ROS generation.

In conclusion, it is abundantly clear that O-GlcNAcylation represents a significant mechanism in the heart's ability to successfully respond to a variety of stressors (Ngoh et al. 2010). Future studies will identify calcium handling and mitochondrial proteins that are O-GlcNAcylated and attempt to elucidate how O-GlcNAcylation mitigates ROS and Ca^{2+} overload in acute MI.

Conflict of interest None of the authors have any conflicts to declare.

References

Akao M, Ohler A, O'Rourke B, Marban E (2001) Mitochondrial ATP-sensitive potassium channels inhibit apoptosis induced by oxidative stress in cardiac cells. Circ Res 88:1267–1275

Ambrosio G, Becker LC, Hutchins GM, Weisman HF, Weisfeldt ML (1986) Reduction in experimental infarct size by recombinant human superoxide dismutase: insights into the pathophysiology of reperfusion injury. Circulation 74:1424–1433

Bernardi P, Scorrano L, Colonna R, Petronilli V, Di Lisa F (1999) Mitochondria and cell death. Mechanistic aspects and methodological issues. Eur J Biochem 264:687–701

Bueno OF, De Windt LJ, Tymitz KM, Witt SA, Kimball TR, Klevitsky R, Hewett TE, Jones SP, Lefer DJ, Peng CF, Kitsis RN, Molkentin JD (2000) The MEK1-ERK1/2 signaling pathway promotes compensated cardiac hypertrophy in transgenic mice. EMBO J 19:6341–6350

Champattanachai V, Marchase RB, Chatham JC (2007) Glucosamine protects neonatal cardiomyocytes from ischemia–reperfusion injury via increased protein-associated O-GLcNAc. Am J Physiol Cell Physiol 292:C178–C187

Champattanachai V, Marchase RB, Chatham JC (2008) Glucosamine protects neonatal cardiomyocytes from ischemia–reperfusion injury via increased protein O-GLcNAc and increased mitochondrial Bcl-2. Am J Physiol Cell Physiol 294:C1509–C1520

Chi L, Tamura Y, Hoff PT, Macha M, Gallagher KP, Schork MA, Lucchesi BR (1989) Effect of superoxide dismutase on myocardial infarct size in the canine heart after 6 hours of regional ischemia and reperfusion: a demonstration of myocardial salvage. Circ Res 64:665–675

Condorelli G, Roncarati R, Ross J Jr, Pisani A, Stassi G, Todaro M, Trocha S, Drusco A, Gu Y, Russo MA, Frati G, Jones SP, Lefer DJ, Napoli C, Croce CM (2001) Heart-targeted overexpression of caspase3 in mice increases infarct size and depresses cardiac function. Proc Natl Acad Sci USA 98:9977–9982

Crompton M (1999) The mitochondrial permeability transition pore and its role in cell death. Biochem J 341:233–249

Crompton M, Costi A, Hayat L (1987) Evidence for the presence of a reversible Ca^{2+}-dependent pore activated by oxidative stress in heart mitochondria. Biochem J 245:915–918

Crow MT, Mani K, Nam YJ, Kitsis RN (2004) The mitochondrial death pathway and cardiac myocyte apoptosis. Circ Res 95:957–970

Di Lisa F (2001) Mitochondrial contribution in the progression of cardiac ischemic injury. IUBMB Life 52:255–261

Di Lisa F, Menabo R, Canton M, Barile M, Bernardi P (2001) Opening of the mitochondrial permeability transition pore causes depletion of mitochondrial and cytosolic NAD^+ and is a causative event in the death of myocytes in postischemic reperfusion of the heart. J Biol Chem 276:2571–2575

Fulop N, Marchase RB, Chatham JC (2007) Role of protein O-linked *N*-acetyl-glucosamine in mediating cell function and survival in the cardiovascular system. Cardiovasc Res 73:288–297

Girffiths EJ, Halestrap AP (1995) Mitochondrial non-specific pores remain closed during cardiac ischaemia, but open upon reperfusion. Biochem J 307:93–98

Girod WG, Jones SP, Sieber N, Aw TY, Lefer DJ (1999) Effects of hypercholesterolemia on myocardial ischemia–reperfusion injury in LDL receptor-deficient mice. Arterioscler Thromb Vasc Biol 19:2776–2781

Halestrap AP (2004a) Does the mitochondrial permeability transition have a role in preconditioning? Circulation 110:e303 (author reply e303)

Halestrap AP (2004b) The mitochondrial permeability transition pore in reperfusion injury and cardioprotection. Cardiovasc J S Afr 15:S5

Halestrap AP (2006) Calcium, mitochondria and reperfusion injury: a pore way to die. Biochem Soc Trans 34:232–237

Haltiwanger RS, Grove K, Philipsberg GA (1998) Modulation of O-linked *N*-acetylglucosamine levels on nuclear and cytoplasmic proteins in vivo using the peptide O-GLcNAc-beta-*N*-acetylglucosaminidase inhibitor O-(2-acetamido-2-deoxy-D-glucopyranosylidene)amino-*N*-phenylcarbamate. J Biol Chem 273: 3611–3617

Hoffmeyer MR, Scalia R, Ross CR, Jones SP, Lefer DJ (2000a) PR-39, a potent neutrophil inhibitor, attenuates myocardial ischemia–reperfusion injury in mice. Am J Physiol Heart Circ Physiol 279:H2824–H2828

Hoffmeyer MR, Jones SP, Ross CR, Sharp B, Grisham MB, Laroux FS, Stalker TJ, Scalia R, Lefer DJ (2000b) Myocardial ischemia/reperfusion injury in NADPH oxidase-deficient mice. Circ Res 87:812–817

Housley MP, Udeshi ND, Rodgers JT, Shabanowitz J, Puigserver P, Hunt DF, Hart GW (2009) A PGC-1alpha-O-GLcNAc transferase complex regulates FoxO transcription factor activity in response to glucose. J Biol Chem 284:5148–5157

Hunter DR, Haworth RA (1979) The Ca^{2+}-induced membrane transition in mitochondria. III. Transitional Ca^{2+} release. Arch Biochem Biophys 195:468–477

Jones SP, Girod WG, Granger DN, Palazzo AJ, Lefer DJ (1999a) Reperfusion injury is not affected by blockade of P-selectin in the diabetic mouse heart. Am J Physiol 277:H763–H769

Jones SP, Girod WG, Palazzo AJ, Granger DN, Grisham MB, Jourd'Heuil D, Huang PL, Lefer DJ (1999b) Myocardial ischemia–reperfusion injury is exacerbated in absence of endothelial cell nitric oxide synthase. Am J Physiol 276:H1567–H1573

Jones SP, Trocha SD, Strange MB, Granger DN, Kevil CG, Bullard DC, Lefer DJ (2000) Leukocyte and endothelial cell adhesion molecules in a chronic murine model of myocardial reperfusion injury. Am J Physiol Heart Circ Physiol 279:H2196–H2201

Jones SP, Trocha SD, Lefer DJ (2001a) Pretreatment with simvastatin attenuates myocardial dysfunction after ischemia and chronic reperfusion. Arterioscler Thromb Vasc Biol 21:2059–2064

Jones SP, Trocha SD, Lefer DJ (2001b) Cardioprotective actions of endogenous IL-10 are independent of iNOS. Am J Physiol Heart Circ Physiol 281:H48–H52

Jones SP, Girod WG, Marotti KR, Aw TY, Lefer DJ (2001c) Acute exposure to a high cholesterol diet attenuates myocardial ischemia–reperfusion injury in cholesteryl ester transfer protein mice. Coron Artery Dis 12:37–44

Jones SP, Gibson MF, Rimmer DM 3rd, Gibson TM, Sharp BR, Lefer DJ (2002) Direct vascular and cardioprotective effects of rosuvastatin, a new HMG-CoA reductase inhibitor. J Am Coll Cardiol 40:1172–1178

Jones SP, Hoffmeyer MR, Sharp BR, Ho YS, Lefer DJ (2003a) Role of intracellular antioxidant enzymes after in vivo myocardial ischemia and reperfusion. Am J Physiol Heart Circ Physiol 284:H277–H282

Jones SP, Greer JJ, van Haperen R, Duncker DJ, de Crom R, Lefer DJ (2003b) Endothelial nitric oxide synthase overexpression attenuates congestive heart failure in mice. Proc Natl Acad Sci USA 100:4891–4896

Jones SP, Teshima Y, Akao M, Marban E (2003c) Simvastatin attenuates oxidant-induced mitochondrial dysfunction in cardiac myocytes. Circ Res 93:697–699

Jones SP, Greer JJ, Kakkar AK, Ware PD, Turnage RH, Hicks M, Van Haperen R, De Crom R, Kawashima S, Yokoyama M, Lefer DJ (2004) Endothelial nitric oxide synthase overexpression attenuates myocardial reperfusion injury. Am J Physiol Heart Circ Physiol 286:H276–H282

Jones SP, Greer JJ, Ware PD, Yang J, Walsh K, Lefer DJ (2005) Deficiency of iNOS does not attenuate severe congestive heart failure in mice. Am J Physiol Heart Circ Physiol 288:H365–H370

Jones SP, Zachara NE, Ngoh GA, Hill BG, Teshima Y, Bhatnagar A, Hart GW, Marban E (2008) Cardioprotection by *N*-acetylglucosamine linkage to cellular proteins. Circulation 117:1172–1182

Kelly BD, Hackett SF, Hirota K, Oshima Y, Cai Z, Berg-Dixon S, Rowan A, Yan Z, Campochiaro PA, Semenza GL (2003) Cell type-specific regulation of angiogenic growth factor gene expression and induction of angiogenesis in nonischemic tissue by a constitutively active form of hypoxia-inducible factor 1. Circ Res 93:1074–1081

Kilgore KS, Friedrichs GS, Johnson CR, Schasteen CS, Riley DP, Weiss RH, Ryan U, Lucchesi BR (1994) Protective effects of the SOD-mimetic SC-52608 against ischemia/reperfusion damage in the rabbit isolated heart. J Mol Cell Cardiol 26:995–1006

Lefer DJ, Granger DN (2000) Oxidative stress and cardiac disease. Am J Med 109:315–323

Lefer DJ, Scalia R, Jones SP, Sharp BR, Hoffmeyer MR, Farvid AR, Gibson MF, Lefer AM (2001) HMG-CoA reductase inhibition protects the diabetic myocardium from ischemia–reperfusion injury. Faseb J 15:1454–1456

Lemasters JJ, Nieminen AL, Qian T, Trost LC, Elmore SP, Nishimura Y, Crowe RA, Cascio WE, Bradham CA, Brenner DA, Herman B (1998) The mitochondrial permeability transition in cell death: a common mechanism in necrosis, apoptosis and autophagy. Biochim Biophys Acta 1366:177–196

Liu J, Marchase RB, Chatham JC (2007a) Glutamine-induced protection of isolated rat heart from ischemia/reperfusion injury is mediated via the hexosamine biosynthesis pathway and increased protein O-GLcNAc levels. J Mol Cell Cardiol 42:177–185

Liu J, Marchase RB, Chatham JC (2007b) Increased O-GLcNAc levels during reperfusion lead to improved functional recovery and reduced calpain proteolysis. Am J Physiol Heart Circ Physiol 293:H1391–H1399

Lucchesi BR, Werns SW, Fantone JC (1989) The role of the neutrophil and free radicals in ischemic myocardial injury. J Mol Cell Cardiol 21:1241–1251

McCord JM (2000) The evolution of free radicals and oxidative stress. Am J Med 108:652–659

Murata M, Akao M, O'Rourke B, Marban E (2001) Mitochondrial ATP-sensitive potassium channels attenuate matrix Ca^{2+} overload during simulated ischemia and reperfusion: possible mechanism of cardioprotection. Circ Res 89:891–898

Nagy T, Champattanachai V, Marchase RB, Chatham JC (2006) Glucosamine inhibits angiotensin II-induced cytoplasmic Ca^{2+} elevation in neonatal cardiomyocytes via protein-associated O-linked *N*-acetylglucosamine. Am J Physiol Cell Physiol 290:C57–C65

Ngoh GA, Jones SP (2008) New insights into metabolic signaling and cell survival: the role of O-GLcNAc. J Pharmacol Exp Ther 327(3):602–609

Ngoh GA, Watson LJ, Facundo HT, Dillmann W, Jones SP (2008) Non-canonical glycosyltransferase modulates post-hypoxic cardiac myocyte death and mitochondrial permeability transition. J Mol Cell Cardiol 45:313–325

Ngoh GA, Facundo HT, Hamid T, Dillmann W, Zachara NE, Jones SP (2009a) Unique hexosaminidase reduces metabolic survival signal and sensitizes cardiac myocytes to hypoxia/reoxygenation injury. Circ Res 104:41–49

Ngoh GA, Hamid T, Prabhu SD, Jones SP (2009b) O-GlcNAc signaling attenuates ER stress-induced cardiomyocyte death. Am J Physiol Heart Circ Physiol 297:H1711–H1719

Ngoh GA, Facundo HT, Zafir A, Jones SP (2010) O-GlcNAc signaling in the cardiovascular system. Circ Res 107:171–185

Palazzo AJ, Jones SP, Girod WG, Anderson DC, Granger DN, Lefer DJ (1998a) Myocardial ischemia–reperfusion injury in CD18- and ICAM-1-deficient mice. Am J Physiol 275:H2300–H2307

Palazzo AJ, Jones SP, Anderson DC, Granger DN, Lefer DJ (1998b) Coronary endothelial P-selectin in pathogenesis of myocardial ischemia–reperfusion injury. Am J Physiol 275:H1865–H1872

Scalia R, Gooszen ME, Jones SP, Hoffmeyer M, Rimmer DM 3rd, Trocha SD, Huang PL, Smith MB, Lefer AM, Lefer DJ (2001) Simvastatin exerts both anti-inflammatory and cardioprotective effects in apolipoprotein E-deficient mice. Circulation 103:2598–2603

Sharp BR, Jones SP, Rimmer DM, Lefer DJ (2002) Differential response to myocardial reperfusion injury in eNOS-deficient mice. Am J Physiol Heart Circ Physiol 282:H2422–H2426

Teshima Y, Akao M, Li RA, Chong TH, Baumgartner WA, Johnston MV, Marban E (2003a) Mitochondrial ATP-sensitive potassium channel activation protects cerebellar granule neurons from apoptosis induced by oxidative stress. Stroke 34(7):1796–1802

Teshima Y, Akao M, Jones SP, Marban E (2003b) Uncoupling protein-2 overexpression inhibits mitochondrial death pathway in cardiomyocytes. Circ Res 93:192–200

Teshima Y, Akao M, Jones SP, Marban E (2003c) Cariporide (HOE642), a selective Na^{+}-H^{+} exchange inhibitor, inhibits the mitochondrial death pathway. Circulation 108:2275–2281

Wang G, Liem DA, Vondriska TM, Honda HM, Korge P, Pantaleon DM, Qiao X, Wang Y, Weiss JN, Ping P (2005) Nitric oxide donors protect murine myocardium against infarction via modulation of mitochondrial permeability transition. Am J Physiol Heart Circ Physiol 288:H1290–H1295

Yang J, Jones SP, Suhara T, Greer JJ, Ware PD, Nguyen NP, Perlman H, Nelson DP, Lefer DJ, Walsh K (2003) Endothelial cell overexpression of fas ligand attenuates ischemia–reperfusion injury in the heart. J Biol Chem 278:15185–15191

Yang S, Zou LY, Bounelis P, Chaudry I, Chatham JC, Marchase RB (2006) Glucosamine administration during resuscitation improves organ function after trauma hemorrhage. Shock 25:600–607

Zachara NE, O'Donnell N, Cheung WD, Mercer JJ, Marth JD, Hart GW (2004) Dynamic O-GlcNAc modification of nucleocytoplasmic proteins in response to stress: a survival response in mammalian cells. J Biol Chem 279:30133–30142

Zou L, Yang S, Hu S, Chaudry IH, Marchase RB, Chatham JC (2007) The protective effects of PUGNAc on cardiac function after trauma-hemorrhage are mediated via increased protein O-GLcNAc levels. Shock 27:402–408

Zou L, Yang S, Champattanachai V, Hu S, Chaudry IH, Marchase RB, Chatham JC (2009) Glucosamine improves cardiac function following trauma-hemorrhage by increased protein O-GLcNAcylation and attenuation of NF-{kappa}B signaling. Am J Physiol Heart Circ Physiol 296:H515–H523